

# HOW CORE STIFFNESS AND POISSON RATIO AFFECT ENERGY BALANCE ROLL STRUCTURE FORMULAS

J. D. Pfeiffer and W. Y. Hamad

Department of Mechanical Engineering

McGill University, Montreal

Quebec, Canada

## ABSTRACT

The stiffness of the core determines how much support it will offer for the initial wraps of web material, and whether this support will be maintained as internal pressures are developed. An expression is developed for calculating the effective modulus of the core for isotropic and anisotropic material. The linear solution is carried further to predict how this core modulus is reflected in local radial hardness of the roll when additional material is wound onto the core. The radial modulus parameters of a roll winding model based upon energy balance are adjusted to account for the stiffening or yielding effect of the core under given winding conditions. The effect of different Poisson ratios on core stiffness and roll formation is discussed.

## NOMENCLATURE

- $c_1, c_2$  = Ratio of inner to outer radii of (1) core, and (2) roll material
- $E_t$  = Tangential modulus of elasticity, Pa or psi
- $E_r$  = Radial modulus of elasticity, Pa or psi
- $\epsilon_t$  = Tangential strain, dimensionless
- $\epsilon_r$  = Radial strain, dimensionless
- $\nu$  = Tangential Poisson ratio, ratio of  $\epsilon_r$  to  $\epsilon_t$  when uniaxial tangential stress is applied
- $k$  = Anisotropy ratio, square root of  $E_t/E_r$
- $K_1, K_2, K_3$  = Coefficients for the equation  $P = -K_1 + K_1 \text{EXP}(K_2 \cdot \epsilon_r) + K_3 \cdot \epsilon_r$   
Units:  $K_1, K_3$  pressure in Pa or psi,  $K_2$  dimensionless,  $P$  interlayer pressure in Pa or psi
- $p$  = pressure applied at the inner radius of core or roll material, Pa or psi
- $q$  = pressure applied at the outer radius of core or roll material, Pa or psi

- $U_r$  = Radial deformation, meters or inches
- $\sigma_t$  = Tangential stress, Pa or psi.
- $\sigma_r$  = Radial stress, Pa or psi.

## INTRODUCTION

Those who write about cores often say that cores are the beginning of the winding process. But to those who use products wound on cores, it is the other way around. Cores are what is left over at the end when all the useful product has expired. Material is often wasted near the core when experience indicates that in terms of web breaks and wrinkles, it is not cost effective to unwind every bit of the roll. Time lost for cleaning up after a web break or culling out products containing wrinkles makes it inadvisable to run the risk. To make the users happy, there should not be any substantial amount of that product left on the core at the end which cannot be used. When a roll is wound, the weight of the roll may be completely supported on the core as it is during centerwinding, or part of the weight may rest on winding drums during surface winding. However, when the roll is unwound it is almost always supported at the core, where the tightness of winding must be sufficient to resist slippage of layers when torque is applied to keep tension on the web. So the core marks one boundary on roll conditions, just as the outside of the roll is the other boundary. Defects which may be attributed to roll structure are particularly likely to occur at either boundary, and in order to thoroughly understand the roll structure near the core, we must know how to incorporate the mechanical properties of the core into roll structure models.

## CORE RADIAL STIFFNESS

When a uniform external pressure is applied to a core tube, the resulting radial deformation could be defined in relation to the force as a spring rate, but it is more convenient to treat the core stiffness as an equivalent modulus, which is the ratio of the applied pressure to the strain created at the tube outer radius. If the test pressure is  $q$ , the effective core modulus  $E_c$  is

$$E_c = \frac{q}{\epsilon_r} = \frac{q b}{U_r} \quad (1)$$

where  $\epsilon_r$  is the radial strain caused by the deformation, or the radial deformation  $U_r$  divided by the radius  $b$  in Figure 1.

A formula for the radial deformation  $U_r$  as a function of internal pressure  $p$  and external pressure  $q$  has been developed by S. G. Lekhnitskii (1), and is given below in its complete form, although here we are interested only in the deformation due to an external pressure.

$$U_r = \frac{b}{E_t(1-c_1^{2k})} \left[ (pc_1^{k+1} - q)(k-v) \left(\frac{r}{b}\right)^k + (p - qc_1^{k-1}) c_1^{k+1} (k+v) \left(\frac{b}{r}\right)^k \right] \quad (2)$$

Where:  $c_1 = \frac{a}{b}$ ,  $k = \sqrt{\frac{E_t}{E_r}}$ ,  $a \leq r \leq b$ ,

and  $\nu = \text{Tangential Poisson ratio}$

By setting  $r = b$ , the external radius, and making  $p$ , the internal pressure zero,  $U_r$  becomes

$$U_r = \frac{b}{E_t(1-c_1^{2k})} [-q(k-\nu) + (-qc_1^{2k})(k+\nu)] \quad (3)$$

which further simplifies to

$$U_r = -\frac{bq}{E_t} \left[ \frac{k(1-c_1^{2k})}{(1-c_1^{2k})} - \nu \right] \quad (4)$$

The minus sign indicates that the deflection is inward, as expected. Formula (4) allows us to calculate the effective core modulus  $E_c$  as a function of the ratio of inner to outer radii for any core material including those with dissimilar properties in the tangential and radial directions ( $k > 1$ ), provided that  $E_t$  and  $E_r$  can be evaluated, which is not always an easy matter for fiber tube cores (2) Note that the assumption of zero pressure on the interior of the core assumes that the interior wall is unsupported by any other rigid body. If there is contact with a stiff inside cylinder the determination of exterior deflection becomes more complex.

By combining equations (1) and (4) the ratio of  $E_c$  to  $E_t$  may be expressed as:

$$\frac{E_c}{E_t} = \frac{1}{\frac{k(1+c_1^{2k})}{(1-c_1^{2k})} - \nu} \quad (5)$$

This relationship is graphed in Figures 1 & 2 against  $a/b$ , the ratio of inner to outer radius, for linear isotropic materials (such as steel or aluminum), using Poisson ratios of zero and 0.3 (Fig. 2) and for linear anisotropic materials with Poisson ratio 0.1 and  $k$  values of 2, 4, and 8 (Fig. 3). The highest value of  $k$  might be taken as appropriate for a model for spiral wound paper tube cores where  $E_t$  is on the order of 4.2 MPa (600,000 psi), however this material is known to be non-linear in compression, so  $k$  will be a function of pressure.

The Poisson ratio acts to stiffen the core against deflection from external pressure as shown in Fig. 2. Here the modulus is increased by 43% when the Poisson ratio goes from 0 to 0.3. Additional strains are produced in the tangential and axial directions when there is a finite Poisson ratio. These strains are proportional to the radial strain caused by external pressure. The net effect is to reduce the radial deformation, which results in a higher effective modulus. On the other hand, the

distribution of radial and tangential stresses inside the ring is a function only of the geometry,  $k$ , and the internal and external pressure, as predicted by the following two equations (6) which do not incorporate  $\nu$  (1):

$$\begin{aligned}\sigma_r &= \frac{pc_1^{k+1} - q}{1-c_1^{2k}} \left(\frac{r}{b}\right)^{k-1} - \frac{p - qc_1^{k-1}}{1-c_1^{2k}} c_1^{k+1} \left(\frac{b}{r}\right)^{k+1} \\ \sigma_t &= \frac{pc_1^{k+1} - q}{1-c_1^{2k}} k \left(\frac{r}{b}\right)^{k-1} + \frac{p - qc_1^{k-1}}{1-c_1^{2k}} kc_1^{k+1} \left(\frac{b}{r}\right)^{k+1}\end{aligned}\quad (6)$$

In the isotropic case, Fig. 2, when  $k=1$ , these equations become the same as the Lamé' solution (3), and are shown here as equation set (7). The stresses within the cylinder then vary as a function of  $1/r^2$ , as is the case of a hollow shaft over which a hub is press-fit.

$$\begin{aligned}\sigma_r &= \frac{pc_1^2 - q}{1-c_1^2} - \frac{p - q}{1-c_1^2} c_1^2 \left(\frac{b}{r}\right)^2 \\ \sigma_t &= \frac{pc_1^2 - q}{1-c_1^2} + \frac{p - q}{1-c_1^2} c_1^2 \left(\frac{b}{r}\right)^2\end{aligned}\quad (7)$$

When the core material is anisotropic, with tangential modulus  $k^2$  times as high as the radial modulus, the rate of change of effective core modulus with radius ratio is greatly reduced, as shown in Fig. 3. When the radial modulus is low compared to the tangential modulus, a small amount of radial deformation will cause inward strains that produce like amounts of tangential strain. In the presence of a high tangential modulus, these strains will cause large tangential stresses, causing annular rings of the material to act as buttresses to support the external pressure so it does not penetrate deeply into the underlying layers. In Fig. 3 at  $a/b = 0.80$  (wall thickness 20% of the outer radius), little if any increase in modulus occurs if the wall thickness is increased to 35% (making  $a/b = 0.65$ ). This shows that it does not pay to add material to the inside of the core because little of the external load is carried on the inner layers.

## SENSING THE PRESENCE OF THE CORE THROUGH LAYERS OF WOUND MATERIAL

Once the numerical value of the core modulus has been obtained, the next logical question is how the hardness (or softness) of the core material will be obscured by the buildup of roll material over it. This information is required in order to program the radial variation of the hardness effect into a roll winding model. Intuitively, one would expect such a curve of hardness to start with the core stiffness modulus at core radius, then change quickly with radius, and finally end up at many multiples of the roll radius with a value approaching that of the roll material itself. Initial attempts to develop such a relationship began with stack testing of layers of roll material and various percentages of a harder, core-type material. The results showed quickly that it was almost impossible to transfer the results of stack tests to the axisymmetric cylindrical geometry of the roll. The next approach was to develop a linear model with isotropic properties, which could be checked

against known solutions in cylindrical coordinates, such as the equations for shrink-fitting a hub on a shaft. Finally, this model was expanded to include anisotropic properties in the core and roll body.

Finite element modeling was used to obtain some numerical solutions for the linear isotropic condition, Fig. 4. The analysis was done on SDRC I-deas software running on a Hewlett-Packard 350 workstation. A test pressure  $q_t$  was applied to the outer circumference of the model. The effective modulus at radius  $c$  was determined by multiplying pressure  $q_t$  times  $c$  divided by the deformation  $U_c$ . The results are reported in Table 1. The general arrangement for a two-body core and roll material model is diagrammed in Fig. 5. Again, the radial deformations  $U_c$  and  $U_b$  result from the test pressure  $q_t$ , applied at radius  $c$ .

Equation (2) will allow the determination of the radial deformations for the model in Fig. 5 provided that external and internal pressures  $q$  and  $p$  can be established for each ring. To obtain the missing information, two sets of equations must be solved using the boundary conditions for each ring. For the inner ring, the internal pressure  $p$  is zero, while the external pressure  $q_b$  is that developed at the interface when the deformation becomes  $U_b$  (at  $r=b$ ). For the outer ring, the external pressure  $q_t$  is the test pressure applied, and the internal pressure at the interface,  $p_b$  exactly equals  $q_b$  for the inner ring. Also, the outer ring's radial deformation at the interface radius  $b$  is equal to that of the inner ring. Note that the variable  $c_1$  in equation (2) applies when  $r$  is between  $a$  and  $b$ , and is to be replaced by  $c_2 = b/c$  when  $r$  is between  $b$  and  $c$ . The variable  $b$  in equation (2) refers to the outer radius, and  $c$  should be used in its place in the case of the outer ring. By setting the two  $U_b$  deformations equal, the following solution is obtained for  $p_b$ , the pressure at the interface, in response to an external pressure  $q_t$ :

$$p_b = q_t \frac{2k_2 c_2^{k_2-1}}{1 - c_2^{2k_2}} \left[ \frac{k_2(1 + c_2^{2k_2})}{1 - c_2^{2k_2}} + \nu_2 \right] + \frac{E_{T2}}{E_{T1}} \left[ \frac{k_1(1 + c_1^{2k_1})}{1 - c_1^{2k_1}} - \nu_1 \right] \quad (8)$$

The deflection at the core may be found using equation (4) with  $q=p_b$ , and the deflection at  $c$  is obtained from equation (2) with  $q=q_t$  and  $p=p_b$ . The answers for a test case, with a solid core with radius  $b=1$ ,  $E_{T1} = 30 \times 10^6$  psi,  $\nu_1 = 0.292$ ,  $E_{T2} = 100,000$  psi,  $\nu_2 = 0.05$ ,  $q_t = 100$  psi, and both  $k$ 's = 1.0 is presented in Table 1, together with the values obtained by finite element analysis of the same problem. The accuracy of the algebraic solution is confirmed by the close agreement with the finite element program results.

The modulus values reported in Table 1 are decreasing with greater distance from the core, as anticipated. For large radius ratios, it was expected that the asymptote would approach the roll material value. (It should approach  $100000/(1-\nu) = 105,263$  psi). The pressure at the core, however, keeps rising as the radius ratio grows, arriving at 1.8 times the test pressure when  $c_2 = 4$ . This is an artifact of the isotropic condition; when winding actual materials one seldom finds equal radial and tangential moduli. Using the analytical approach several more test cases can be solved for different anisotropy ratios, and the results are plotted in Figs. 6 and 7.

Here an aluminum core is modeled, having  $\nu_1$  ratio = 0.8, a modulus of 107 psi and  $\nu_1 = 0.334$ . The roll material tangential modulus is kept at a constant value of 600,000 psi, typical of both paper and polyester film, while the radial modulus is found by dividing this value by  $k^2$ . The Poisson ratio of the roll material is assumed to be 0.20, the tangential value. This may seem to be abnormally high, but remember that the radial value,  $\nu_r$  will be  $\nu_t$  divided by  $k^2$ , which will agree with the range of values typically measured during stack tests of compressible sheet material.

Fig. 6 shows that the ability to detect the presence of a hard core by modulus measurements made at the outside surface becomes all but impossible at radius ratios of 2.5 or greater, whenever  $k$  is 8 or greater. This is within the normal range of  $k$  values for paper and many plastic film materials. The range of  $k$  from 2 to 8 would apply to plastic film materials with very high  $E_r$  modulus, and especially those with low  $E_t$  modulus, on the order of 150 000 psi. Winding materials having  $E_r = 600$  000 psi at the same time  $E_t$  has the same value are hard to find. However, soft polyethylene film with  $E_t$  of about 25 000 psi can be wound tightly enough to make  $E_r$  have this same value, with behavior represented in Fig. 7 where  $k=1$ .

It is important to realize that these curves, though interesting and informative, do not solve the problem of predicting adjustments for roll material stiffness parameters. The curves are limited to predicting, in a linear anisotropic material of constant radial modulus, how strongly the core properties can be sensed at different distances from the core. Fig. 6 gives an appreciation of how rapidly the effect can fade away when  $k$  is large, but this is not the whole story of what happens when the roll is wound. The initial layers which are added over a hard core also present a hard interface to the layers added, because of the stiffening effect of the core underneath. It would be extremely complicated to develop a predictor equation which takes into account the continuous change of  $k$  with radius as more layers are added.

## MODIFICATIONS TO ENERGY BALANCE ROLL STRUCTURE FORMULAS

The energy balance scheme (4.5) does not require repeated iteration of the winding structure from the core outward every time an incremental thickness of wind is added to the outer radius. Instead, a single pass is made to calculate the roll residual interlayer pressure and tangential stress, beginning at the outer radius and moving to the core. The energy in a unit volume of web is calculated, based on the winding tension and the  $E_t$  modulus of the web. This energy appears inside the roll body as a combination of the energy necessary to produce non-linear compression of the sheet material up to the interlayer pressure, and the energy associated with the residual tangential stress within the roll. The combination is calculated using the distortion energy theory (5) The rate of change of pressure with radius,  $d\sigma_r/dr$ , is limited by the hoop stress equation (9) to be that which is allowable under the current values of  $\sigma_r$  and  $\sigma_t$  to keep the equation in balance.

$$-\sigma_r - r \frac{d\sigma_r}{dr} + \sigma_t = 0 \quad (9)$$

The solution proceeds directly from the outer radius of the roll to the core radius, making evaluations of the winding tension level at every iteration step and halfway between steps (Runge-Kutta integration is employed). Nothing mentioned so far in the description of the energy balance solution method gives the program a warning that the stiffening effect of the core is soon to be felt. Indeed, the normal progress of the solution is such that if the winding tension values are available, it will continue to calculate down to a radius of zero without ever acknowledging the presence of a core. In fact, the residual pressure value when this former solution method reached core radius is called the "no-core" pressure  $P_0$ , which will be employed later.

### USING RADIAL STIFFNESS MULTIPLIERS TO ACCOUNT FOR CORE STIFFENING

The approach that is recommended to work with the energy balance solution is patterned on how the web actually responds during winding in the zone adjacent to the core. The first several wraps laid against a hard metal core cannot easily be moved radially by the pressure developed by wraps laid in top. If they could deform radially inward toward the roll center, the rapidly changing tangential strain would cause them to lose their initial tension, just as wraps in the outer roll body do. But the stiffness of the core prevents them from moving inward, so they behave as if their  $E_r$  radial modulus has been artificially increased by the presence of the core.

$E_r$  for the roll body is found by taking the derivative of the pressure vs strain equation (6), equation (10), with respect to strain  $\epsilon_r$ . Equation (11) for  $E_r$  is most readily evaluated if the strain  $\epsilon_r$  is known. To solve for strain when the pressure is known, evaluate equation (12) and set  $\epsilon_r^{(0)} = \epsilon_r^{(1)}$ . Do this several times until  $\epsilon_r^{(0)}$  and  $\epsilon_r^{(1)}$  are essentially equal. With  $\epsilon_r^{(0)}$  beginning at zero, the convergence is rapid.

$$P = -K_1 + K_1 e^{k_2 \epsilon_r} + K_3 \epsilon_r \quad (10)$$

$$E_r = \frac{dP}{d\epsilon_r} = K_1 k_2 e^{k_2 \epsilon_r} + K_3 \quad (11)$$

$$\epsilon_r^{(1)} = \frac{1}{K_2} \log \left( \frac{P + K_1 - K_3 \epsilon_r^{(0)}}{K_1} \right) \quad (12)$$

The multiplier  $\gamma$  is used to raise or lower  $E_r$ . It is used on both  $K_2$  and  $K_3$ , but not  $K_1$ . The form for calculating  $\gamma$  is given in equation (14).

$$P = -K_1 + K_1 e^{\gamma k_2 \epsilon_r} + \gamma K_3 \epsilon_r \quad (13)$$

$$\gamma = 1 + \frac{F_1}{(R - \beta)^9} \quad (14)$$

The slope  $E_r$  of equation (13), defined as in equation (11), will be  $K_1 \gamma K_2 \cdot \text{EXP}(\gamma K_2 \epsilon_r) + \gamma K_3$ . Note that a slope of  $\gamma E_r$  will be achieved at a new  $\epsilon_r$  which is  $1/\gamma$  of the former value. The slope change has been achieved by a  $1/\gamma$  rescaling of the

strain axis which, conveniently, allows reporting the actual strain of a layer near the core by multiplying the calculated  $\epsilon_r$  by  $\gamma$ .  $F_1$ ,  $\beta$  and  $\theta$  in equation (14) are dimensionless quantities which will be determined below. Although  $\theta$  is usually taken as 1, it will be included in the procedure for evaluating the other coefficients in the event other values such as 1.5 or 2 are chosen.  $R$  is the dimensionless ratio of roll radius  $r$  to core radius  $b$ . To model the effects shown in Fig. 6 where  $E_t$  is much greater than  $E_r$  a function is required which will cause a high slope of the stiffness parameter near the core. Equation (14) is capable of modeling this when  $\beta$  is made slightly less than 1, and  $F_1$  is positive. Alternately, when winding on a soft core with  $E_c$  slightly lower than  $E_r$ ,  $F_1$  will be negative to soften the roll body, and  $\beta$  will be considerably less than 1, near zero or negative.  $F_1$  and  $\beta$  depend upon  $\gamma_0$ , which is the value of  $\gamma$  at the core surface, and a slope  $SL$ , which is  $d\gamma/dR$  at the core, and an intercept. The equations for these relationships are given below, where  $P_0$  is the "no-core" pressure that would exist at radius  $b$  if  $\gamma = 1$  for all radii.

$$F_2 = \frac{E_c}{K^2 P_0} \quad (15)$$

$$K^2 = \frac{E_t}{K^2 P_0} \quad (16)$$

$$\gamma_0 = N_1 [1 - \exp(-F_2/N_2)] \quad (17)$$

$$SL = \left[ N_3 + \frac{N_4}{F_2 + N_5} \right] 2 k^2 \quad (18)$$

$$\beta = \frac{\theta(\gamma_0 - 1)}{SL} + 1 = \frac{(\gamma_0 - 1)}{SL} + 1 \Big|_{\theta = 1} \quad (19)$$

$$F_1 = \frac{SL}{\theta} (1 - \beta)^{(\theta+1)} = -SL (1 - \beta)^2 \Big|_{\theta = 1} \quad (20)$$

Dimensionless empirical constants used above are:  
 $N_1 = 25$        $N_2 = 27.972$        $N_3 = -16.31755$   
 $N_4 = 80.12425$        $N_5 = 4.43017$

Note that  $K^2 \cdot P_0$  has been used in equations (15) and (16) as an approximation to  $E_r$ . This is a shortcut to using equation (11), and the results will be only a few percent low, sufficient for estimation of stiffness parameter effects, especially when constants  $N_1 - N_5$  can be adjusted to compensate. The determination of  $P_0$  is the most difficult step, requiring several iterations to find a balance between the equal quantities  $\sigma_r$  and  $\sigma_t$  just outside the core radius, where we assume  $d\sigma_r/dr$  is zero.

$$P_0^{(0)} = \frac{\sigma_w^2 K^2}{2 E_r} \quad \zeta_w = \frac{\sigma_w^2}{2 E_r} \quad (21)$$



$$P_0 = -K1 + K1 e^{K2\varepsilon} + K3 \varepsilon \quad \sigma_t = \sigma_r = -P_0 \quad (22 a)$$

$$\zeta_r = -K1\varepsilon + \frac{K1}{K2} (e^{K2\varepsilon} - 1) + \frac{K3}{2} \varepsilon^2 \quad (22 b)$$

$$\sigma_e = -\sqrt{2\zeta_r E_T} \quad (22 c)$$

$$\zeta_s = \frac{\sigma_t^2 - \sigma_t \sigma_e + \sigma_e^2}{2 E_T} \quad \zeta_s = \zeta_w ? \quad (22 d)$$

The two parts of equation (21) give an initial approximation for  $P_0$  and evaluate  $\zeta_w$  the unit stored energy due to tensile stress  $\sigma_w$  in the incoming web. Since the tension may be programmed as a function of radius, it should represent the average tension in the zone nearest the core. Equations (22 a-d) are evaluated several times until the unit stored energy  $\zeta_s$  in the zone near the core is sufficiently close to  $\zeta_w$  to stop the iterations. When a new estimate of pressure  $P_0$  is made as defined in (22a), it is also assigned (negatively) to  $\sigma_t$  as the rate of change of pressure with radius is assumed negligibly small here. The energy  $\zeta_r$  involved in compressing the roll material up to strain  $\varepsilon_r$  is found by the closed form of the integral of  $P$  vs  $\varepsilon_r$  equation (22b). But to calculate the total stored energy on a distortion-energy basis, an equivalent stress  $\sigma_e$  must be calculated using equation (22c), a stress which is scaled similarly to  $\sigma_t$  and which is a linear equivalent of the non-linear compression response. Then the stored energy  $\zeta_s$  is calculated and compared to  $\zeta_w$  in equation (22d). Steps a) through d) are repeated until the difference is very small, a procedure which takes much less time in computer cycles than it takes to describe.

## ROLL WINDING EXAMPLES

The empirical constants in equations (17) to (20) were developed by fitting results to some known solutions to roll winding problems which use the method developed by Dr. Z. Hakiel (7). His winding model re-balances all of the residual stresses throughout the roll on each iteration of adding tensile wraps at the outside, and in this manner it is able to take into account the stiffening action of the core. In the four examples under consideration, the tension was assumed to have no variation with roll radius (constant tension winding). Core stiffness  $E_c$  values were rounded off after having been calculated according to equation (5). Polynomial coefficients  $C_0, C_1, C_2, \dots$  are those of the series  $E_r = C_0 + C_1 \cdot P^1 + C_2 \cdot P^2, \dots$ , the preferred form for handling non-linear compression in the Hakiel solution. The values of  $K1, K2, K3$  to reproduce the same  $P$  vs  $\varepsilon$  behavior were obtained by curve-fitting the polynomial series. Note that  $C_1$  and  $K2$  are roughly equal.

The one-pass energy balance method solution for these four cases is shown as a solid line in Figures 8a through 11b. In each the radial pressure diagram is shown on the left and residual tension  $\sigma_t$  is shown on the right part of the Figure. The solutions produced by the previous version of the method, without correction for core effects is shown by the curves labeled  $\gamma=1$ .

Fig. 8 corresponds to a condition where a high  $K2$ - or high  $C1$ - polyester-type plastic film is wound on a hollow metal core. The material parameters agree with

those used in an example by Dr. Hakiel published in 1989 (7). The condition represented by Fig. 9 is more typical of paper wound on a metal core.

The material properties demonstrated in Fig. 10 are similar to those of Fig. 8, except for the inclusion of a high  $C_0$  term in the polynomial expression, and the fact that winding takes place at a lower constant tension. The example is from a recent publication by A. Penner (8). In Fig. 11 a moderately stiff polyester film is wound tightly on a fiber core, causing large amounts of core deformation and the formation of high negative tangential stress just above the core. The energy balance solution method prints out a warning message near the inflection point of Fig. 11 b) at radius ratio 1.3 that buckling is likely to occur.

## CONCLUSIONS

The inclusion of the anisotropy ratio in formulas for the radial deformation of core structures and linear axisymmetric models makes possible the prediction of effects due to the application of pressure from the outside and the reaction from the underlayers which present a resistance to deformation. The abrupt attenuation of pressure disturbances with radius whenever  $k$  values higher than 2 are encountered confirms the premise under which the energy balance roll structure programs were developed: that energy admitted to the roll does not migrate substantially in radial distance from the location at which it was applied. Residual pressure and tangential stress patterns for several widely different cases agree well with the best known analytical solutions. This agreement may be further improved as more data becomes available to refine the five dimensionless constants used to adjust the local effective  $E_r$  for the presence of the core. The multiplier which adjusts  $K_2$  and  $K_3$  for stiffening effects is available to restore them for reporting on the true amount of radial strain at any position within the roll.

## ACKNOWLEDGMENTS

The authors wish to thank Dr. Z. Hakiel for providing solutions to roll structure problems, and the Web Handling Research Center at Oklahoma State University for additional computational assistance.

## REFERENCES

1. Lekhnitskii, S. G., Anisotropic Plates, Gordon and Breach, Inc., New York, 1968, pp. 106-108.
2. Gerhardt, T. D., "External Pressure Loading of Spiral Paper Tubes: Theory and Experiment", Transactions of the ASME, Vol. 112, April 1990, pp. 144-150.
3. Timoshenko, S., Theory of Elasticity, Maple Press, York, Pa., 1938, p. 57.
4. Pfeiffer, J. D. "Prediction of Roll Defects from Roll Structure Formulas", TAPPI Journal, Vol. 62, No. 10, Oct. 1979 pp. 83-85.
5. Pfeiffer, J. D. "An Update of Pfeiffer's Roll-Winding Model", TAPPI Journal, Vol. 70, No. 10, Oct. 1987, p. 132.
6. Pfeiffer, J. D. "Surface Winding to Overcome the Strain Deficiency", TAPPI Journal, Vol. 73, No. 10, Oct. 1990, pp. 247-250.

7. Hakiel, Z. "Nonlinear Model for Wound Roll Stresses", TAPPI Journal, Vol. 70, No. 5, May 1987, pp. 113-117.
8. Penner, A. "Roll Structure Calculations at Constant Wound-In Tension", TAPPI Proceedings. 1990 Finishing and Converting Conference, Oct. 1990, pp. 105-110.

**TABLE 1**  
Radial deformations obtained by FEA and analytical solution

Radius c in	Finite element analysis		Analytical solution, equations (2), (4), and (7)			
	Deformation $U_c$ $10^{-3}$ in.	Modulus E at c	Deformation $U_c$ $10^{-3}$ in.	Modulus E at c	Deformation $U_b$ $\mu$ inch	Pressure at b, psi
1.5	0.566	265,018	0.5675	264,306	3.2032	135.73
2.5	1.744	143,349	1.7453	143,239	3.9203	166.12
3.0	2.303	130,265	2.3043	130,193	4.0772	172.76
3.5	2.845	123,023	2.8457	122,994	4.1780	177.04
4.0	3.373	118,589	3.3737	118,563	4.2462	179.92

**TABLE 2**  
Winding parameters: Four cases  
(Note: in all four cases the value of  $E_t$  is 600 000 psi)

Case	$E_c$ , psi	$\sigma_w$ , psi	CO	C1	C2	K1	K2	K3
1	890 000	333.33	0	1060	-0.153	0.059600	1049.88	-19.625
2	890 000	555.55	0	124	0.0	0.056124	124.006	0.1875
3	890 000	300.0	1060	1060	0.0	0.968729	1056.299	-88.75
4	46 000	1000.0	0	450	0.0	0.056109	450.036	0.75

**TABLE 3**  
Parameter determination for stiffness multiplier  $\gamma$

Case	$P_0$ , psi	$\gamma_0$	SL	$\beta$	$F_t$
1	125.83	5.35115	-83.052	0.9476093	0.279598
2	34.13	24.9864	-4520.85	0.9946943	0.127264
3	106.03	6.18263	-105.474	0.9508633	0.254658
4	497.44	0.18297	5.183	0.8423482	-0.128806

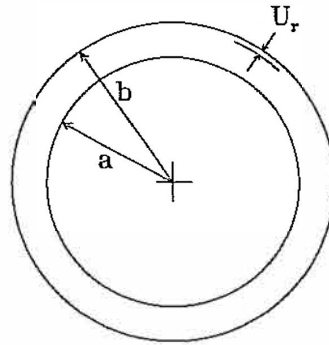


Fig. 1 Core dimensions.  $a$  = core inner radius  $b$  = outer radius. Ratio  $c_1 = a/b$   
 $U_r$  = radial deformation.

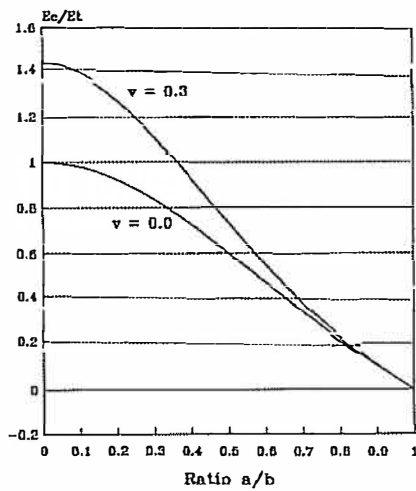


Fig. 2 Ratio of core effective modulus to elastic modulus vs. ratio of inner to outer radius for isotropic, linear materials with Poisson ratio 0.0 and 0.3.

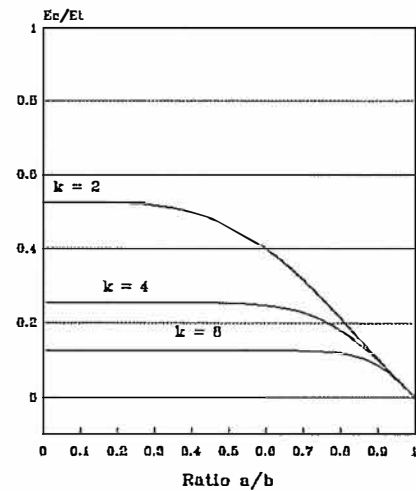


Fig. 3 Ratio of core modulus to elastic tangential modulus vs  $a/b$  ratio for anisotropic linear materials with  $k$  values of 2, 4 and 8, with Poisson ratio = 0.1 for all three cases.

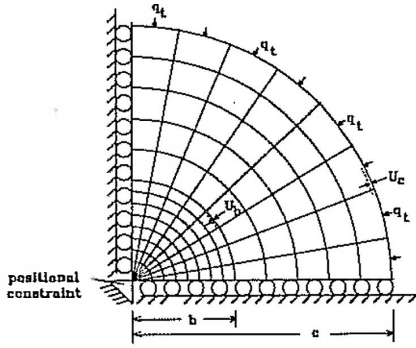


Fig. 4 Finite element model used to find radial deformations at core/roll interface and at roll outer radius under linear isotropic conditions. Circles indicate frictionless constraint at edges.

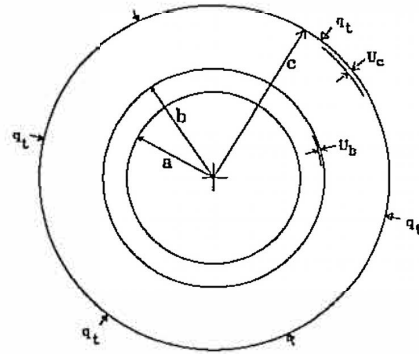


Fig. 5 Diagram of core and roll model. Radial deformations  $U_c$  and  $U_b$  are measured at roll outer radius and core outer radius, respectively.  $c_1$  ratio =  $a/b$ ,  $c_2$  ratio =  $b/c$ .

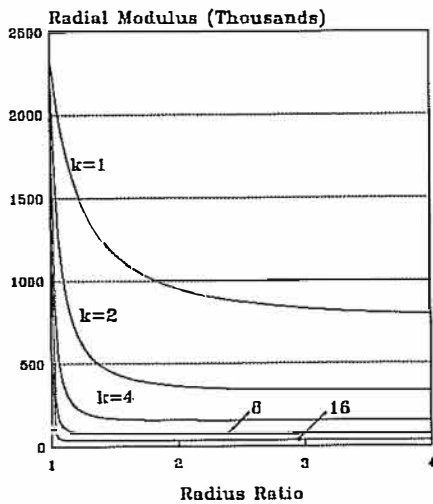


Fig. 6 Variation of radial modulus with distance from core for various ratios of  $k$ . Core aluminum,  $a=0.8$ ,  $b=1$ . Roll material  $E_t = 600,000$  psi,  $v_t = 0.2$ ,  $E_r$  values depend upon  $k$ .

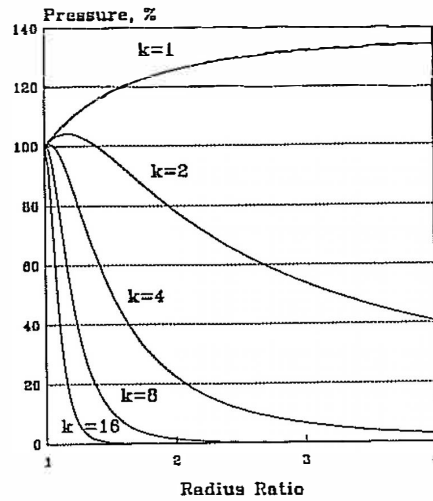


Fig. 7 Percentage of externally applied pressure reaching core vs. radius ratio for various values of ratio  $k$ .

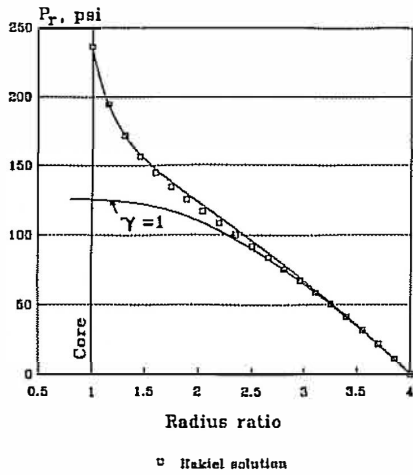


Fig. 8 a) Pressure vs. radius ratio for case 1 (7).  $\gamma=1$  curve assumes no core effects are present

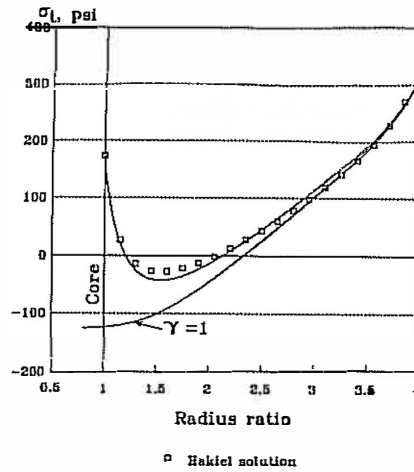


Fig. 8 b) Residual tangential stress vs. radius for case 1.

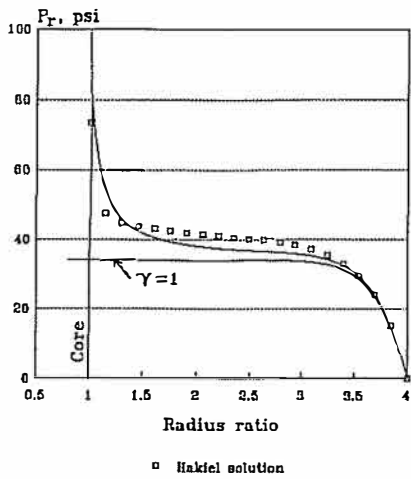


Fig. 9 a) Radial pressure vs radius ratio for case 2.

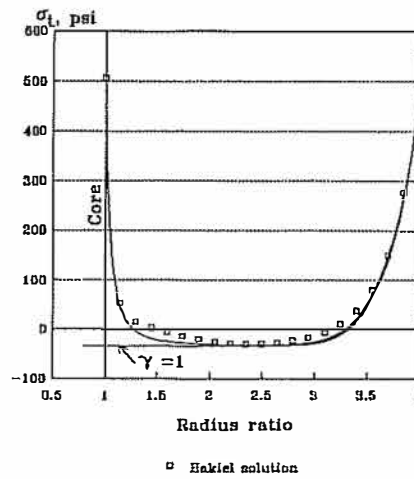


Fig. 9 b) Tangential stress vs radius ratio for case 2.

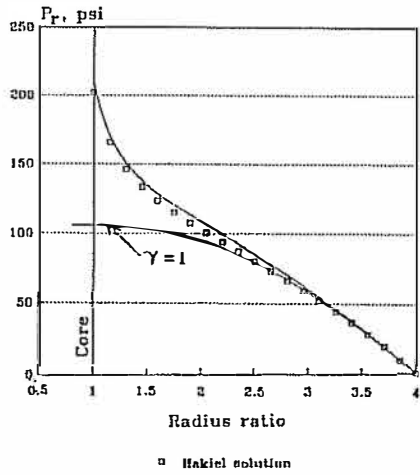


Fig. 10 a) Radial pressure vs radius ratio for case 3.

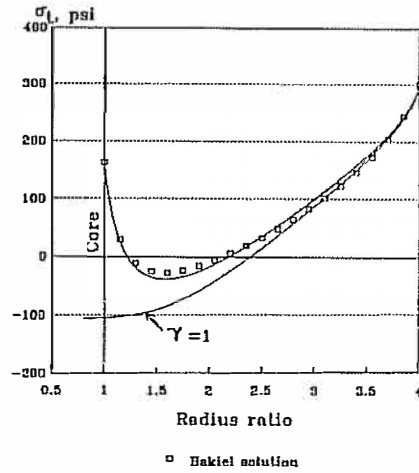


Fig. 10 b) Tangential stress vs radius ratio for case 3.

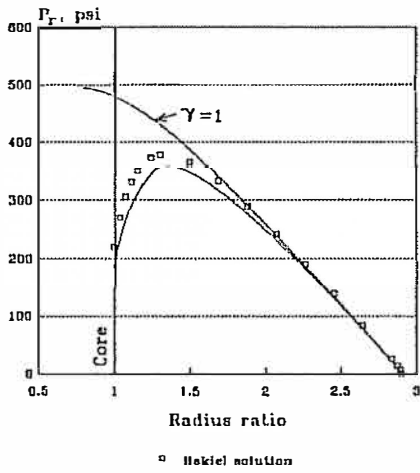


Fig. 11 a) Radial pressure vs radius ratio for case 4.

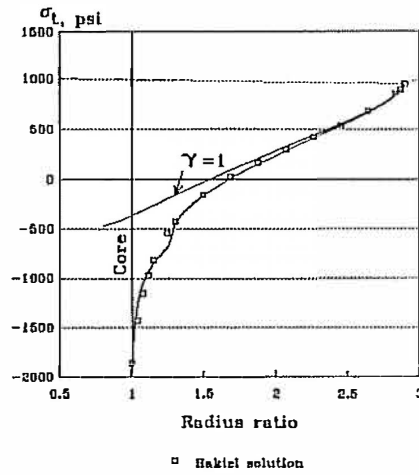


Fig. 11 b) Tangential stress vs radius for case 4.

## HOW CORE STIFFNESS AND POISSON RATIO AFFECT ENERGY BALANCE ROLL STRUCTURE FORMULAS

David Pfeiffer

**What is the Physical Origin/significance of the “Stiffening Factor”  $\gamma$  ?**  
Zig Hakiel, Kodak

Thank you Dr. Hakiel. The origin of it is that the layers as they are wound actually sense or feel the pressure of a stiff core material underneath or conversely a soft core material underneath. If you lay the first wrap of winding against a steel rod no amount of external pressure is going to shrink that first wrap significantly, and you must shrink it radially a significant distance to spill away its tension. If you don't spill away its tension, its tension will remain high no matter what you put on the outside of it, so the only way to account for that is to locally increase the modulus because the modulus is that of the package. The radial deflection of the paper layer that is being stressed by layers wound on top is supported by what is underneath, and what is underneath is a combined package of some pieces of core and some layers of paper that are next to the core. As you go outward, the effect fades away, when you get further way from the core pipe that is the heart of the roll. So it is a physical situation, and if you modeled enough simultaneous equation solutions based on it, the gamma function would fall out. Your own solution Dr. Hakiel, takes it into account automatically by looking at the incremental solution of applying a wrap on the outside of the roll and how that changes the tangential stress of each subsequent wrap underneath of it, and those wraps that are up against the solid core don't change their tangential stress very much at all, and therefore remain with their initial winding tension in them. Essentially the ones closest to the core have the initial tension and the ones a little further away begin to have their tension reduced until you reach a minimum amount of tension at a certain distance from the core. Anyway, there is a physical significance to  $\gamma$ . It's the incremental hardness change or response change to the radial compression of the material based on the presence or absence of a stiff core at some proximity to where you are putting on the material.

**Core stiffness is a function of winding angle, i.e. both  $E_t$  and  $\nu_{r\theta}$  are functions of this angle. Can Lekhnitski's equation incorporate changes in  $\nu_{r\theta}$  with winding angle?**

Terry Gerhardt, Sonoco

That's a good question. In the first order, I think it can. He in his book Anisotropic Plates went into things on a axisymmetric basic without a winding angle, but I don't think it would take too much work to stretch the theory to account for the change of properties with the winding angle of the spiral of winding tube cores for instance. It wouldn't be directly applicable; you would have to work out that effect. I think the formulas published so far would allow you to combine those two. I didn't take that as my assignment. I was trying to get a more general set of equations to handle a wider range of conditions.